# Unweighted event generation in hadronic $WZ$ production at order $(\alpha_S)$

Matt Dobbs* and Michel Lefebvre†
*Department of Physics and Astronomy, University of Victoria, P.O. Box 3055, Victoria, British Columbia, Canada V8W 3P6*
(Received 24 November 2000; published 8 February 2001)

We present an algorithm for unweighted event generation in the partonic process $pp \to W^{\pm}Z(j)$ with leptonic decays at next-to-leading order in $\alpha_S$. Monte Carlo programs for processes such as this frequently generate events with negative weights in certain regions of phase space. For simulations of experimental data one would like to have unweighted events only. We demonstrate how the phase space from the matrix elements can be combined to achieve unweighted event generation using a second stage Monte Carlo integration over a volume of real emissions (jets). Observable quantities are kept fixed in the laboratory frame throughout the integration. The algorithm is applicable to a broader class of processes and is CPU intensive.

DOI: 10.1103/PhysRevD.63.053011 PACS number(s): 14.70.−e, 02.70.Rr, 12.38.−t

## I. INTRODUCTION

Next-to-leading order in $\alpha_S$ (NLO($\alpha_S$)) corrections in diboson production are large at the CERN Large Hadron Collider (LHC) and sizable at the Fermilab Tevatron (see for example [1,2]). Run I physics analyses (i.e., [3,4]) at the Tevatron have employed constant $k$-factors to approximate NLO($\alpha_S$) corrections. With the increased energy and luminosity of Run II and the new energy regime that will be probed with the CERN LHC, simulations incorporating higher order corrections will be of increased importance.

NLO($\alpha_S$) differential cross section predictions for diboson production at hadron colliders are normally accomplished with Monte Carlo integration programs. Divergences inherent in the Feynman graphs contributing at $\mathcal{O}(\alpha_S)$ are handled with either the phase space slicing method [5] or the subtraction method [6] with the effect that both positive weighted events and negative weighted (or probability) events are generated. The contribution from negative weighted events cancels in an integration over a suitably large volume of hadronic final states, and a physical (positive probability) prediction is obtained. Integration programs are successful in producing distribution and cross section predictions for inclusive observables subject to any experimental cuts providing statistics are large enough to effect the cancellations, and a sufficient volume of jets has been integrated within each histogram bin. However, owing to the negative probability events, unweighted event generation—the generation of events with the distribution predicted by theory—with these NLO($\alpha_S$) matrix elements has not been achieved to date.

Unweighted event generation is often preferred over integrated distributions because it can genuinely simulate experimental data and because it is difficult to perform detector simulation on the large event statistics required for integrated distributions.

Unweighted event generation can be reduced to a problem of rendering all event weights positive definite. If a sample of positive definite weighted events can be obtained, the Monte Carlo hit-and-miss method is commonly used for unweighting. The maximum event weight $d\sigma_{\max}$ for the process is estimated, for instance, by sampling the cross section a number of times. The ratio of event weight over the maximum event weight $d\sigma/d\sigma_{\max}$ is compared to a random number $g$ generated uniformly in the interval (0,1). Events for which the ratio exceeds the random number ($d\sigma/d\sigma_{\max} > g$) are accepted, the others are rejected. This ensures the accepted events are distributed according to the description provided by the matrix element, and so all have unit weight.

In this paper we describe an algorithm which extends the usefulness of the present NLO($\alpha_S$) hadronic di-boson production programs by providing a means for unweighted event generation thereby presenting the NLO($\alpha_S$) predictions in a format better suited for experimental simulations. It deals specifically with the region of low transverse momentum of the $WZ$ system, where higher order corrections are largest. As for the Drell-Yan process, resummation (first proposed by [7]) is expected to give more reliable predictions in this region—however a resummed treatment of the $WZ(j)$ process does not exist and a comparison with fixed order predictions will always be of interest. Another approach for this problematic region is the matching of the zero-order matrix elements using a parton shower model for simulations of the initial-state shower to the first order tree level [i.e., $\mathcal{O}(\alpha_S)$] matrix elements. This has been accomplished for the single vector boson case [8,9].

The algorithm makes use of the matrix elements from the Baur-Han-Ohnemus (BHO) [10] integration package which employs the phase space slicing method as regularization scheme. This scheme makes use of approximations for the analytic integration of a volume of soft and collinear real emissions. The approximations break down before the volume can be increased sufficiently to render all event weights positive.

The algorithm presented here is an extension of the phase space slicing method. A cylinder of jets defined by a transverse momentum cutoff $P^T_{\text{cutoff}}$ is used to partition event generation into a subprocess where the real emission has sufficient transverse momentum to be potentially observable (called 1 jet) and another subprocess (called 0 jet) where the real emission (if present) has sufficiently small transverse momentum such that it is taken as unobservable. There are no divergences in the 1 jet cross section so these events all have positive weights and unweighted event generation may

*Electronic address: matt.dobbs@cern.ch
†Electronic address: lefebvre@uvic.ca

 

be accomplished by applying Monte Carlo hit-and-miss. Difficulties arise in the treatment of the 0 jet events, which is the topic of this paper.

The missing transverse momentum in 0 jet events may arise from the invisible neutrino and from jets which escape detection. By fixing the total missing transverse momentum rather than the individual contributions from the invisible neutrino and unobserved jets, an integration volume of real emissions phase space can be generated and so the cancellations between the real emissions and one-loop graphs can be accomplished by a Monte Carlo integration over this jet volume. The charged lepton and missing transverse momentum vectors (i.e., the observable quantities) are kept fixed in the laboratory frame throughout the integration. Since the jet volume may be large, the fixing of the observable quantities is essential. An integration which instead keeps other quantities such as the subprocess energy and boost fixed (as would be the case if the phase space slicing method were applicable to such large jet volumes) would also necessarily be an integration over observationally different charged lepton vectors.

A final state neutrino is not the only means of generating the missing transverse momentum over which a jet volume can be integrated. Anything which contributes to the missing transverse momentum may be used including the primordial $k^T$ distribution of the proton, multiple interactions, minimum bias events, and even detector resolution. For $WZ$ production with leptonic decays, the invisible neutrino is a convenient choice. In generalizing this algorithm to other processes different contributions to the missing transverse momentum could be used.

Section II of this paper briefly enumerates the presently available integration packages for hadronic $WZ$ production and outlines the regularization schemes commonly used for the matrix elements before describing the algorithm in some detail. In Sec. III cross sections and several differential cross section distributions from integration packages are compared to events generated with this algorithm. Our conclusions are presented in the final section.

## II. ALGORITHM FOR UNWEIGHTED EVENT GENERATION

We choose the specific process $pp \to W^+Z(j)$ with electron/muon-type vector-boson decays as a case study to apply the algorithm. LHC energy is chosen because the challenges in terms of negative probability events are more severe at 14 TeV than for the Tevatron case.

### A. Order $\alpha_S$ cross section

Hadronic $WZ$ production at NLO($\alpha_S$) has been calculated in Refs. [10–13]. All calculations with the exception of Ref. [12] use the narrow width approximation, wherein the gauge bosons are taken on their mass shell. The correlations in the decays of the vector bosons to massless fermions are fully included in Refs. [12,13], while they are included in all but the one-loop graphs in Ref. [10]. For the numerical implementation of the NLO($\alpha_S$) matrix elements Refs. [11–13] use the subtraction method, while Ref. [10] employs the phase space slicing method. The calculations of Refs. [11–13] were found to be in agreement in Ref. [13]. An updated version of the Ref. [10] program incorporating an omitted region of phase space has been compared with Ref. [13] and found to be in good agreement [1, Sec. 5.5].

The NLO($\alpha_S$) cross section receives contributions from the square of the Born level graphs, the interference of the Born graphs with the one-loop graphs, and the square of the real emission graphs,

$$\mathcal{M}^2_{\rm NLO} = \mathcal{M}^2_{\rm Born} + \mathcal{M}_{\rm Born} \otimes \mathcal{M}_{\rm one\ loop} + \mathcal{M}^2_{\rm real\ emission}. \quad (1)$$

Soft, collinear, and ultraviolet divergences appear when any of the $\mathcal{O}(\alpha_S)$ graphs are treated alone, and so a regularization scheme is necessary to ensure the inherent cancellations. The matrix elements used in this study employ the phase space slicing method. A volume of real emissions phase space [herein referred to as (n+1)-body phase space] is partitioned by means of soft and collinear cutoffs[1]. and incorporated analytically with the soft gluon and leading pole approximations into the phase space of the diagrams lacking a real emission (herein referred to as n-body).

In the region where the soft and collinear divergences overlap, the perturbative QCD calculation may be visualized in terms of an expansion in powers of

$$\frac{\alpha_S}{2\pi}\left[\ln\frac{\hat{s}}{P^{T\,2}_{\rm jet}}\right]^2 \quad (2)$$

where $\alpha_S$ is the QCD coupling, $\sqrt{\hat{s}}$ is the subprocess energy and characterizes the scale of the interaction, and $P^T_{\rm jet}$ is the transverse momentum of the order $\alpha_S$ real emission. When the jet transverse momentum $P^T_{\rm jet}$ is small relative to $\sqrt{\hat{s}}$, the function given in Eq. (2) becomes large and multi-gluon emission is important—this is the problem region for fixed order calculations. We wish to integrate out a large enough $P^T_{\rm jet}$ volume such that the function given in Eq. (2) remains smaller than unity. For $\sqrt{\hat{s}}=1$ TeV this gives $P^T_{\rm jet}$ of order 10 GeV, which in turn corresponds nicely to the detector capabilities at the LHC, wherein typically jets above 15 (30) GeV will be reconstructed at low (high) luminosity. Smaller jet integration volumes would be necessary at lower machine energies.

The situation is illustrated schematically in Fig. 1. A hypothetical jet transverse momentum distribution is shown for

[1]The phase space slicing method defines the soft jet region by

$$E^{\rm CMS}_{\rm jet} < \delta_s \frac{\sqrt{\hat{s}}}{2}$$

where $E^{\rm CMS}_{\rm jet}$ is the jet energy in the $WZj$ subprocess center of mass frame, $\delta_s$ is the soft cutoff, and $\sqrt{\hat{s}}$ is the subprocess energy. The collinear region is defined by

$$|E_i E_j \pm \vec{p}_i \cdot \vec{p}_j| < \delta_c \hat{s}$$

where $E_i$ and $\vec{p}_i$ are the energy and momentum of massless parton $i$ and $\delta_c$ is the collinear cutoff. For more details see Ref. [5].

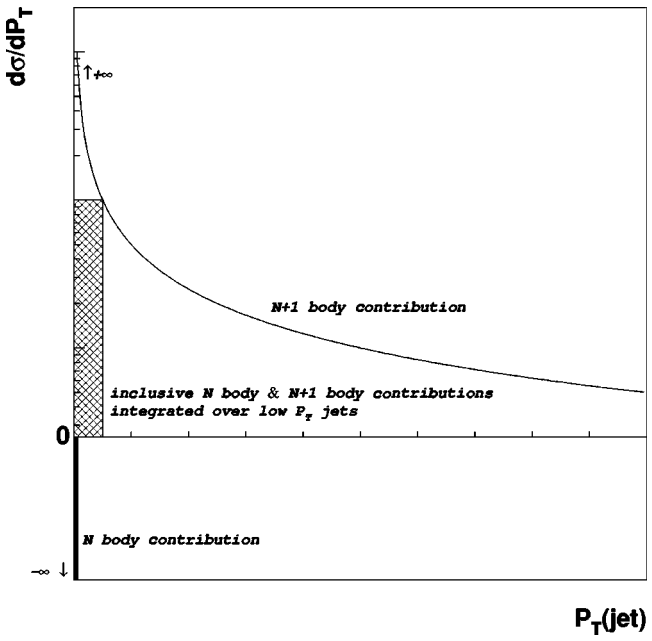


FIG. 1. A hypothetical transverse momentum distribution of the jet $P_{\rm jet}^T$ in the NLO($\alpha_S$) integration is shown for illustrative purposes. The (n+1)-body contribution diverges (solid curve) as $P_{\rm jet}^T \to 0$. The n-body contribution is a negative divergence at the origin. The divergences cancel in the integral over a suitably large volume of hadronic final states (hatched region).

the n-body and (n+1)-body case. The (n+1)-body contribution diverges as the jets become soft or collinear, while the n-body contribution is a negative divergence at the origin. The divergences cancel in an integration over a suitably large volume of jet transverse momenta (hatched region). The phase space slicing method effects such an integration, but the jet volume is not sufficiently large to keep the cross section in the inclusive (hatched) region positive for most events.

### B. Generating unweighted events

We begin by dividing events into two classes: those containing a jet with sufficient transverse momentum ($P_{\rm jet}^T > P_{\rm cutoff}^T$) to be classified as potentially observable (referred to here as 1 jet); and those without a jet or containing a jet with transverse momentum below the cutoff $P_{\rm jet}^T < P_{\rm cutoff}^T$ (referred to as 0 jet). This differs from the definition of n-body and (n+1)-body events where the soft and collinear cutoffs define the partition. In the 1 jet region, the matrix elements are order $\alpha_S$, but the calculation is leading order. There are no divergences nor are there negative weighted events, so event generation can be accomplished with the usual Monte Carlo techniques.

The algorithm concerns events in the 0 jet region only and we focus exclusively on events of this type for the remainder of this paper.

The phase space slicing method is extended by integrating out the cylinder of jets defined by the $P_{\rm cutoff}^T$ using a second stage Monte Carlo integration. As the $P_{\rm cutoff}^T$ is chosen to be the order of 10 GeV, there is a danger that the integration may affect the kinematics of the event to the point which is observable by the detector. With this in mind, the observable vectors (charged leptons for the case of *WZ* production with leptonic decays) are kept fixed throughout the integration, and the center of mass frame vectors are allowed to fluctuate.

We start by sampling the observable quantities of the event i.e., fixing the vectors

$$P_{l_W^\pm}, P_{l_Z^+}, P_{l_Z^-}, \vec{P}_{\rm miss}^T \tag{3}$$

where $P_{l_W^\pm}$ is the momentum of the charged lepton from the $W^\pm$ decay, $P_{l_Z^+}, P_{l_Z^-}$ are the momenta of the charged leptons from the $Z$ decay, and $\vec{P}_{\rm miss}^T$ is the missing transverse momentum. With the $Z$ boson taken on shell and requiring no net momentum transverse to the beam, this amounts to 8 degrees of freedom.

For the case of the n body matrix element these vectors also fix the neutrino four-vector with $\vec{P}_\nu^T = \vec{P}_{\rm miss}^T$ and the $W$-mass constraint gives zero or two solutions for the neutrino longitudinal momentum. Within the BHO matrix elements a further 4 degrees of freedom specify the NLO($\alpha_S$) corrections. Thus the average n body weight $\langle d\sigma^{\text{n-body}} \rangle$ for the observable event is arrived at by integrating over these degrees of freedom and averaging over the two neutrino solutions. This weight is usually negative. When no neutrino solutions exist the weight is zero. We refer to a point in the full n body phase space (defined by the vectors of Eq. (3), the 4 extra degrees of freedom, and the neutrino solution choice) as a ''subevent,'' such that an ''event'' as defined by this algorithm is an integration over many subevents.[2]

We now incorporate the cylinder of jets defined by the $P_{\rm cutoff}^T$ by performing a similar integration over (n+1)-body subevents. For each subevent a jet with transverse momentum up to the cutoff is sampled (3 degrees of freedom). The jet transverse momentum fixes the invisible neutrino transverse momentum for the event with the constraint that the observed missing transverse momentum is kept fixed,

$$\vec{P}_\nu^T = \vec{P}_{\rm miss}^T - \vec{P}_{\rm jet}^T . \tag{4}$$

The longitudinal neutrino momentum is specified up to a two-fold ambiguity by the $W$-mass constraint. The charged lepton vectors are also kept fixed in the laboratory frame, such that all the quantities in Eq. (3) are unchanged throughout the integration. The average subevent weight is $\langle d\sigma^{(\text{n+1})\text{-body}} \rangle$, which is a positive number.

The phase space for a Monte Carlo integration is normally sampled in terms of variables such as the invariant masses, rapidities, and decay angles which give a triangular transformation matrix such that the Jacobian is the product of the diagonal entries (as is the case for the di-boson integration packages). The fixed charged lepton vectors in the laboratory frame constraint introduces inherent correlations, and the transformation matrix becomes more complicated: for the

[2]A subevent from this algorithm corresponds precisely to an event from a Monte Carlo integration package.

$WZ$ 1 jet case it is a $11\times11$ matrix with no zero elements. Fortunately it is simple to calculate this matrix and its Jacobian numerically on an event by event basis, which is the strategy we have used. This Jacobian is included in the subevent weights $d\sigma^{\text{n-body}}$ and $d\sigma^{(\text{n+1})\text{-body}}$.

The total event weight for the configuration defined by Eq. (3) is the sum of the n-body and (n+1)-body contributions, with a factor which accounts for the observable vectors phase space sampling

$$d\sigma^{0\text{ jet}} = W_{\text{phase space}} \times (\langle d\sigma^{\text{n-body}} \rangle + \langle d\sigma^{(\text{n+1})\text{-body}} \rangle). \quad (5)$$

It is unimportant that the number of subevents for the second stage integration be sufficiently large to give an accurate result for each observable event. A poor accuracy simply means two identically configured events may have differing event weights, however by grace of the Monte Carlo method, the average converges to give the correct cross section. The subevent statistics are required to be sufficiently large to ensure the event weights of Eq. (5) very rarely fall negative on account of statistical fluctuations. We refer to events where this occurs as ''remnant negative weight events.'' Events of this type are discarded, and thus contribute to a (biased) systematic Monte Carlo error. The number of subevents is a means of directly controlling this error. It is easy to evaluate this error.

Finally, we note the application of this algorithm to the re-weighting of leading order events [i.e., re-scaling of tree level event weights to account for NLO($\alpha_S$) corrections] needs to be approached with caution, as the phase space volume of observable vectors in Eq. (3) is larger for the (n+1)-body case than for the n body case since only limited configurations of these vectors provide n-body neutrino longitudinal momentum solutions which satisfy the $W$-mass constraint. This difference needs to be accounted for in a re-weighting scheme.

## III. RESULTS AND COMPARISON WITH INTEGRATION PACKAGES

The results presented in this section use identical parameters as the comparison of integration packages in Ref. [1, Sec. 5.5] with the exception of the jet definition for the jet veto. In that study the jet transverse momentum cutoff $P^T_{\text{cutoff}}$ was motivated by what the detectors are capable of measuring. Here we motivate the $P^T_{\text{cutoff}}$ by what the detector is incapable of reconstructing: a $P^T_{\text{cutoff}}$ of 15 GeV is defined to partition the 1 jet and 0 jet regions (there is no jet rapidity requirement). The CTEQ4M [14] structure functions are used. Input parameters are taken as $\alpha_{EM}(M_Z)=\frac{1}{128}$, $\sin^2\theta_W=0.23$, $\alpha_s(M_Z)=0.1116$, $M_W=80.396$ GeV, $M_Z=91.187$ GeV, factorization scale $Q^2=M_W^2$, and Cabibbo angle $\cos\theta_{\text{Cabibbo}}=0.975$ with no 3rd generation mixing. Branching ratios are taken as $\text{Br}(Z\rightarrow l^+l^-)=3.36\%$, $\text{Br}(W^\pm\rightarrow l^\pm\nu)=10.8\%$. The $b$ quark contribution to parton distributions has been taken as zero. Kinematic cuts motivated by anomalous triple gauge boson coupling analyses are chosen (see for example [1, Sec. 5]). The transverse momentum of all charged leptons must exceed 25 GeV and the rapidity of all charged leptons must be less than 3 in magnitude. Missing transverse momentum must be greater than 25 GeV. The BHO package is employed for the evaluation of matrix elements.

We first evaluate the algorithm's ability to integrate out the negative probability events. The second stage integration is accomplished with relatively low statistics to keep the computer processing time reasonable, only 100 subevents of each type [n-body and (n+1)-body] are used.

For the default choices of the soft and collinear cutoffs in the BHO matrix elements ($\delta_s=0.01$, $\delta_c=0.001$) the cancellations between the n-body and (n+1)-body partitions are very large, and the second stage integration would need unreasonably large statistics for good behavior.[3] In order to achieve a portion of the jet volume integration analytically we increase the cutoffs ($\delta_s=0.05$, $\delta_c=0.002$) keeping them well within the range of applicability of the soft gluon and leading pole approximations. We emphasize that experiments must take the integration volume into account by ensuring that their analysis is not sensitive to jets within the volume (as defined by the jet momentum cutoff of this algorithm *and* the soft and collinear cutoffs of the phase space slicing method). This consideration is true in general for the phase space slicing method.

With these choices of the phase space slicing cutoffs ''remnant negative weight events'' account for approximately 0.1% of the total sample of weighted events and $-0.02\%$ of the cross section. Most of these events are the result of the low second stage integration statistics such that re-evaluating these events with a larger number of subevents renders the event weight positive.

There is another class of remnant negative events which are not due to statistics. For these events the charged lepton in the $W$-decay is emitted along the line of flight of the $W$ in its rest frame. This configuration is disfavored by the spin correlations, wherein the $W^+$-decay ($W^-$-decay) with a left-handed (right-handed) particle emitted along the $W$ line of flight is preferred. The BHO matrix elements use a spin averaged treatment for the one-loop graphs and so these correlations are not at all included for the virtual corrections (though spin correlations are included everywhere else). This means events in this configuration receive an unphysically large negative contribution from the one-loop graphs while receiving the correct (spin correlation suppressed) contribution from the other graphs. Thus this class of negative event weights arise as a result of the lepton correlation approximations used in the BHO matrix elements. The algorithm is sensitive to these approximations and would benefit from improved theoretical calculations (as are included in [12,13]). The negative weights associated to events of this type are extremely small.

Finally there are a few events with negative weights at

[3]The same problematic behavior is observed when matrix elements employing the subtraction method are used. We found no immediate solution to this problem for the subtraction method, and so we have been unable to use this algorithm with subtraction method matrix elements thus far.

TABLE I. The integrated cross section subject to the cuts described in the text is compared for the leading order BHO calculation, the NLO($\alpha_S$) BHO calculation, and for this algorithm which uses the BHO matrix elements.

| 0 jet LHC $W^+Z$ production cross section | |
|---|---|
| Baur-Han-Ohnemus LO | $70.5 \pm 0.1$ fb |
| Baur-Han-Ohnemus NLO($\alpha_S$) | $51.0 \pm 0.1$ fb |
| This 2 Stage Algorithm | $50.5 \pm 0.3$ fb |

extraordinary subprocess energy ($\sqrt{\hat{s}} > 5$ TeV) where the total cross section is orders of magnitude below one event per LHC year. These events may arise from a combination of the lepton correlation effect and an insufficiently large jet volume for events at this energy scale, as suggested by the function given in Eq. (2).

### A. Comparison with the BHO integration package

In Table I we enumerate the leading order and NLO($\alpha_S$) predictions for 0 jet $WZ$ production from the BHO integration package together with the result from this algorithm which employs the BHO matrix elements. The NLO($\alpha_S$) prediction differs considerably from the leading order one and this algorithm is able to reproduce the NLO($\alpha_S$) BHO predictions well. The accuracy of the prediction from this algorithm suffers slightly with respect to that from the BHO integration package alone in that the correlations between integration variables make it more difficult for the adaptive integration to optimize the phase space sampling.

It takes considerably more computer time to evaluate the NLO($\alpha_S$) matrix elements than for the leading-order case. This algorithm requires a further factor 200 over the NLO ($\alpha_S$) integration package in evaluating one weighted event because of the $2 \times 100$ subevents in the second stage integration.

Monte Carlo hit-and-miss is used to extract a sample of unweighted events from the (positive definite) events generated using this algorithm. No attempt has been made to optimize for efficiency, and the time required for the generation of one unweighted event is quite large[4] with an efficiency of about 0.1%. Nevertheless it is possible to generate an event sample of a few low luminosity LHC years (i.e., several thousand events) in several hours using computer farms of the size currently in use at most universities or experiments.

Weighted 0 jet event distributions are compared in Figs. 2 and 3 for the BHO integration package and this algorithm. Figure 2 (top) shows the transverse momentum distribution of the $Z$, which is the distribution normally used to probe anomalous $WWZ$ couplings at hadron colliders [16]. The rapidity separation between the $Z$-boson and the charged lepton from the $W$-decay (Fig. 2, bottom) is sensitive to the approximate radiation zero in hadronic $WZ$ production [17]. Finally the missing transverse momentum distribution is shown in Fig. 3. The jet integration volume arises from this distribution, and so it is the place where discrepancies between this algorithm and the integration package might arise. The agreement between the BHO integration package and this algorithm in all of these distributions is good.

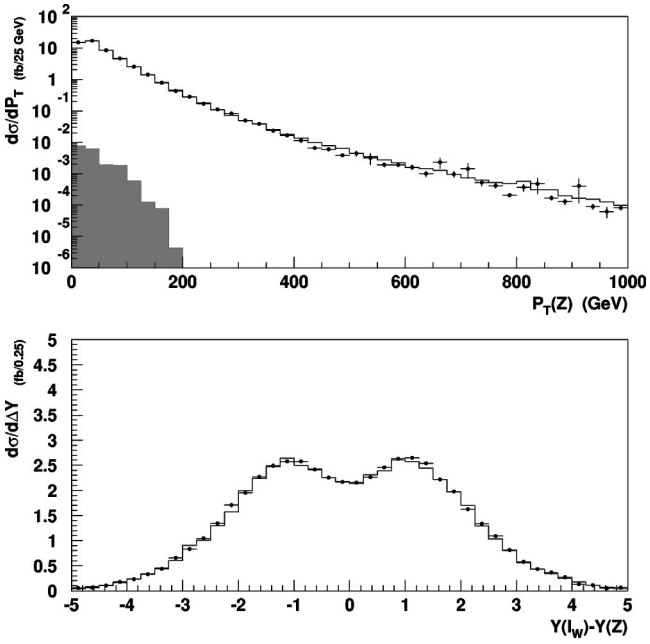


FIG. 2. The transverse momentum distribution of the $Z$ ($P_Z^T$, top) and the rapidity separation between the $Z$ and the lepton from the $W$ decay [$Y(l_W) - Y(Z)$, bottom] are compared for weighted events from the BHO NLO($\alpha_S$) generator (solid open histogram, statistical errors are small) and for weighted events from the algorithm (points with error bars). Only positive weighted events are included in the algorithm distribution, and the errors are statistical only. The distribution of discarded negative weighted events from the algorithm are shown in the lower shaded histogram (using the absolute value of the weights). This distribution is several orders of magnitude below the positive weight event distribution, and is only observable on the logarithmic upper plot. The distributions are for the 0 jet case with kinematic cuts as described in the text.

In order to evaluate the effect of remnant negative weight events, the absolute value of the weights of negative events is plotted in Figs. 2 and 3 (shaded regions). The remnant negative weight event distribution is several orders of magnitude below the positive event distribution in all cases and is largest in the region where the differential cross section is also largest, and so the effect of these events is negligible everywhere. Histograms of this sort provide the means of evaluating the effect of these remnant negative events. For faster event generation the second stage integration statistics may be decreased, resulting in an increase in the size of this shaded region. It is impossible to completely eliminate the shaded region of remnant negative events by increasing the second stage integration statistics indefinitely, due to the lepton correlation effects discussed in the first part of this section. If the negative weighted events from the BHO integra-

[4]200 seconds are required for one unweighted event using a 600 MHz personal computer running Linux 2.2. PYTHIA [15] requires only about 0.02 seconds for the generation of one leading order $WZ$ event with an efficiency of 1–2 %.

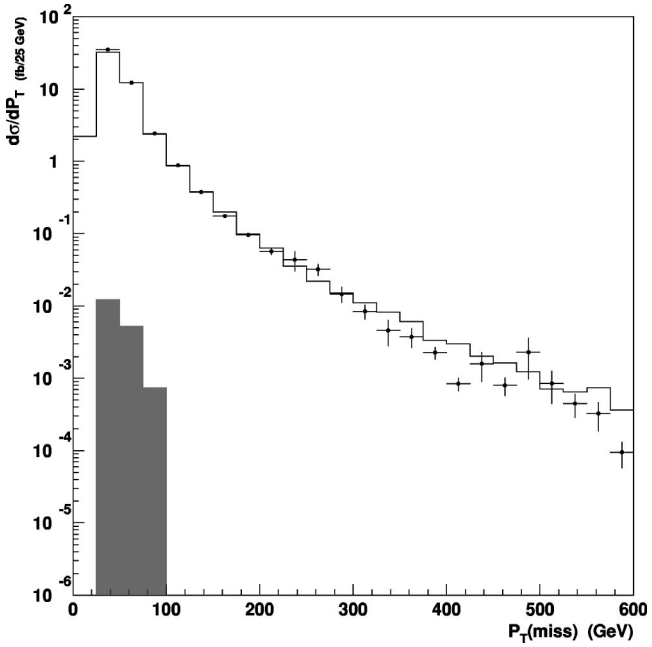


FIG. 3. The missing transverse momentum distribution $P^T_{\rm miss}$ is compared for weighted events from the BHO NLO($\alpha_S$) generator (solid open histogram, statistical errors are small) and for weighted events from the algorithm (points with error bars). Only positive weighted events are included in the algorithm distribution, and the errors are statistical only. The distribution of discarded negative weighted events from the algorithm are shown in the lower shaded histogram (using the absolute value of the weights). This distribution is several orders of magnitude below the positive weight event distribution. The distribution is for the 0 jet case with kinematic cuts as described in the text.

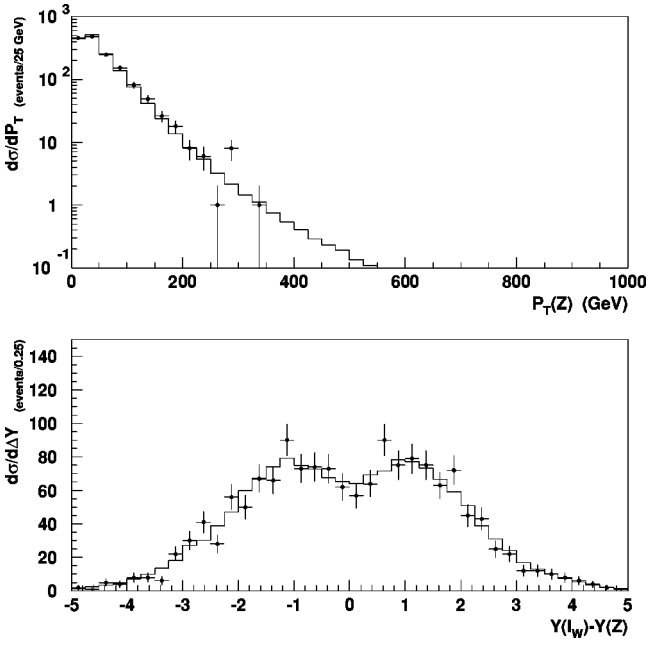


FIG. 4. The transverse momentum distribution of the $Z$ ($P^T_Z$, top) and the rapidity separation between the $Z$ and the lepton from the $W$ decay [$Y(l_W)-Y(Z)$, bottom] are compared for weighted events from the BHO NLO($\alpha_S$) generator (solid open histogram, statistical errors are small) and for unweighted events from the algorithm (points with error bars). The distributions are for an integrated luminosity corresponding to three years of low luminosity running at the LHC (30 fb$^{-1}$). The error bars assume Poisson statistics. The distributions are for the 0 jet case with kinematic cuts as described in the text.

tion package (without this algorithm) were also superimposed, they would be distributed uniformly about half an order of magnitude below the BHO prediction.

In Fig. 4 unweighted events from this algorithm are superimposed on the BHO integration package prediction for the same distributions as Fig. 2. The error bars assume Poisson statistics and the agreement is good. This figure represents the first unweighted event generation at NLO($\alpha_S$) for the partonic process $pp \to WZ(j)$.

## IV. CONCLUSIONS

We have described an algorithm for unweighted event generation at NLO($\alpha_S$) for the partonic process $pp \to WZ(j)$ with leptonic decays and evaluated its effectiveness at LHC energy. Event generation consists of a two stage Monte Carlo integration, and so requires considerable computer time. The possibility of optimizing the generation and the code itself has not been addressed, and certainly the performance may be considerably improved. The partition of events into 0 jet and 1 jet regions is motivated by experimental capabilities and defined by a jet transverse momentum cutoff. This partition, as well as the n-body and (n+1)-body partition inherent in the phase space slicing method, must be taken into account in experimental analyses.

Generation of high transverse momentum real emissions is not addressed by this algorithm, but this region of events is free of divergences and so unweighted event generation is easily achieved with the usual Monte Carlo methods.

A small number of remnant negative weighted events are discarded by the algorithm. The effect of these events is negligible and contributes to a biased systematic Monte Carlo error which may be monitored and evaluated.

The agreement between events generated with this algorithm and the BHO NLO($\alpha_S$) integration package is good.

The algorithm is generalizable to a broader class of processes. Hadronic $W\gamma(j)$ production can be treated in an identical way, while the $W^+W^-(j)$ process with leptonic decays can be handled by treating the neutrino (anti-neutrino) as invisible and the anti-neutrino (neutrino) as an observable lepton for the purposes of this algorithm. Other means of generating the jet integration volume besides the invisible neutrino may be used for other processes.

## ACKNOWLEDGMENTS

The authors would like to thank the ATLAS Collaboration which motivated this project. We are grateful to Ulrich Baur for providing the matrix elements as well as informative correspondence and discussions. We thank Ian Hinchliffe and Jørgen Beck Hansen for useful comments. This work has been supported by the Natural Sciences and Engineering Research Council of Canada.

[1] S. Haywood *et al.*, in Electroweak Physics, Proceedings of the Workshop on Standard Model Physics (and more) at the LHC, Geneva, Switzerland, 1999, edited by G. Altarelli and M.L. Mangano, CERN-2000-004, hep-ph/0003275.
[2] U. Baur *et al.*, ''Report of the working group on photon and weak boson production,'' hep-ph/0005226.
[3] D0 Collaboration, S. Abachi *et al.*, Phys. Rev. D **56**, 6742 (1997).
[4] D0 Collaboration, B. Abbott *et al.*, Phys. Rev. D **60**, 072002 (1999).
[5] H. Baer, J. Ohnemus, and J.F. Owens, Phys. Rev. D **40**, 2844 (1989).
[6] R.K. Ellis, D.A. Ross, and A.E. Terrano, Nucl. Phys. **B178**, 421 (1981).
[7] Y.L. Dokshitzer, D. Diakonov, and S.I. Troian, Phys. Rep. **58**, 269 (1980).
[8] G. Miu and T. Sjöstrand, Phys. Lett. B **449**, 313 (1999).
[9] G. Corcella and M.H. Seymour, Nucl. Phys. **B565**, 227 (2000)
[10] J. Ohnemus, Phys. Rev. D **44**, 3477 (1991); U. Baur, T. Han, and J. Ohnemus, *ibid.* **51**, 3381 (1995).
[11] S. Frixione, P. Nason, and G. Ridolfi, Nucl. Phys. **B383**, 3 (1992).
[12] J.M. Campbell and R.K. Ellis, Phys. Rev. D **60**, 113006 (1999).
[13] L. Dixon, Z. Kunszt, and A. Signer, Nucl. Phys. **B531**, 3 (1998); Phys. Rev. D **60**, 114037 (1999).
[14] H.L. Lai *et al.*, Phys. Rev. D **55**, 1280 (1997).
[15] T. Sjöstrand, Comput. Phys. Commun. **82**, 74 (1994).
[16] D. Zeppenfeld and S. Willenbrock, Phys. Rev. D **37**, 1775 (1988).
[17] U. Baur, T. Han, and J. Ohnemus, Phys. Rev. Lett. **72**, 3941 (1994).